ICAS 2016
30th Congress of the International Council of the Aeronautical Sciences
DCC, Daejeon, Korea ; September 25-30, 2016

NUMERICAL STUDY ON TRANSONIC BUFFET ACTIVE CONTROL BY OPEN AND CLOSED-LOOP STRATEGIES

Chuanqiang Gao, Weiwei Zhang, Zhengyin Ye
*** School of Aeronautics, Northwestern Polytechnical University, Xi'an 710072, China**

Abstract

Oscillating aerodynamic loads induced by transonic buffet may cause structural fatigue and flight accidents, making transonic buffet control a hot topic in aeronautical engineering. In this paper, two active control strategies (open-loop and closed-loop) are proposed to decrease or suppress the transonic buffet by trailing edge flap based on Unsteady Reynolds-averaged Navier–Stokes equations and Spalart–Allmaras turbulence model. The buffet loads can be reduced by 60% with the open-loop strategy, and the buffet in a wider range of Mach numbers can be suppressed completely with the closed-loop strategy.

1 Introduction

Transonic buffet [1-4] is an aerodynamic phenomenon that leads to a self-sustained motion of the shock. Buffet limits the flight envelope of an aircraft and may lead to structural fatigue or even flight accidents. Therefore, transonic buffet and transonic buffet control have elicited considerable research interests in aviation.

With the development of CFD, the Reynolds-averaged Navier–Stokes (RANS) method based on turbulence models has gained much attention to simulate transonic buffet. Most researchers [5-12] adopted Unsteady Reynolds-averaged Navier–Stokes (URANS) equations to study the unsteady characteristics. Previous research has shown that the accuracy of numerical calculations is mainly determined by the accuracy of the turbulence model. Goncalves [7] studied various turbulence models, and found that URANS equations based on Spalart–Allmaras (SA) turbulence model could predict the main properties of buffet flow.

Transonic buffet control is divided into passive and active controls. Passive control strategy is to change the boundary layer environment, such as shock control bump [13-13], and vortex generators [16, 17]. These methods can alleviate shock wave oscillation to a certain extent, which aim to postpone buffet onset and reduce buffet unsteady loads. However, passive control has two limitations: first, the controller merely works in default states, while in other states, the controller may damage aerodynamic performance; second, most passive control methods can only alleviate buffet but cannot cancel it out. As an active control strategy, trailing edge deflector (TED) [18-19] attempted to change the airfoil trailing edge environment to achieve buffet control. In a wind tunnel experiment, Caruana [18] studied the effect of static actuated positions of TED on the buffet onset with an open-loop strategy. TED can increase the aerodynamic performance (generally refers to the lift) and delay the buffet onset. Further study indicated that TED could decrease the buffet loads to some extent, under a closed-loop control law using the feedback of unsteady wall static pressure [19]. TED can also be considered as the evolution of flap. Doerffer [3] and Barbut [20] conducted an experimental study and numerical simulation of transonic buffet flow around a wing with periodic oscillating flap. The effects of the flap actuation have been studied in two cases, illustrating that the periodic oscillating flap with one-third of the buffet frequency could decrease the buffet loads. Such open-loop control strategy has an obvious shortcoming, that is, it requires uninterrupted

and large amounts of energy pumped into the actuator to ensure the flap rotation in the designed amplitude and frequency. Generally speaking, the above mentioned active control methods have achieved some progress in the exploration of buffet control. However, there is a common shortcoming of these methods that they can't completely suppress buffet.

This study proposes a open-loop and a closed-loop control strategy for transonic buffet suppression. NACA0012 airfoil with 20% of the airfoil chord flap is adopted. First, the buffet onsets and buffet loads of the stationary airfoil are verified with experimental data based on URANS equations and SA turbulence model. Second, the possibility of the flap actuation driven by an open-loop and a closed-loop strategies are investigated.

2 Unsteady buffet flow simulations

The test case of the transonic buffet simulations follows the wind tunnel transonic buffet tests by Doerffer [3]. They performed a wind tunnel test on a NACA0012 airfoil at Mach numbers from 0.7 to 0.8, at Reynolds numbers of 3 10^6, and within a range of angles of attack that include the buffet onset.

In the current study, transonic buffet simulations of the NACA0012 airfoil were performed with the finite volume method [21]. The algorithm used in this study is the AUSM+up algorithm. The turbulence model used is the SA turbulence model. The details of the simulation method and the validations can be referred to the Ref. [10,12,21], in which the effects of the time step and the grid were investigated. The predicted buffet onset, buffet frequency and buffet loads match well with the experimental data.

The computational domain is covered by a hybrid unstructured grid. The far field extends about 20 chords away from the airfoil. There are 25361 surface nodes, and 40 boundary layers around the airfoil. The distance between the first layer and the wall in the perpendicular direction is 5×10^{-6} chords ($y^+ \sim 1$). The physical time step adopted in the present study is 2.94 10^{-4}s. Figure 1 shows the time histories of the aerodynamic forces at M = 0.7 and $\alpha = 5.5^\circ$. Figure 2 shows the power spectrum densities (PSD) of the lift coefficient and the moment coefficient. It can be seen that the buffet frequency is 0.2 in the nondimensional reduced frequency scale. The reduced buffet frequency is defined as $k_b = \frac{\pi f_b c}{U_\infty}$, where f_b is the buffet frequency; c indicates the chord of the airfoil; and U_∞ denotes the velocity of the free-stream.

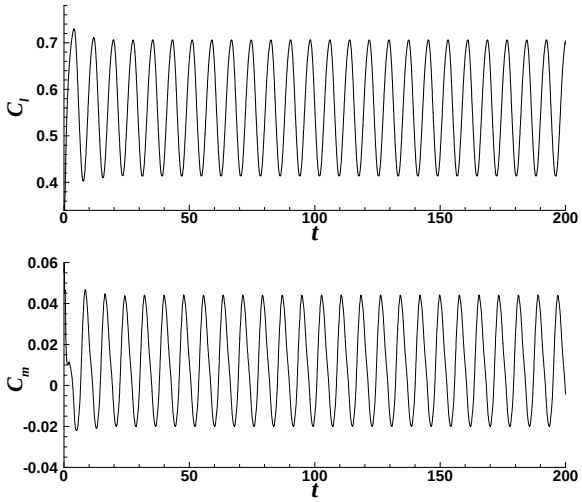

Figure 1. Evolution of lift and moment coefficients at angle of attack of 5.5 and M=0.7

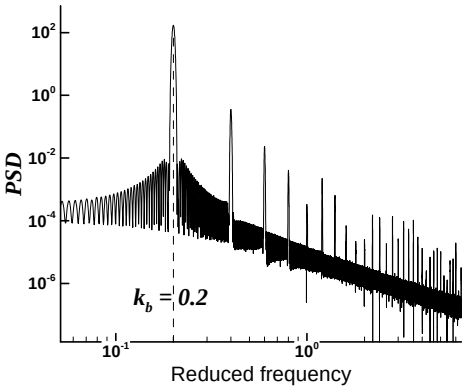

Figure 2. Power spectrum density analyses of the aerodynamic responses at M=0.7 and $\alpha = 5.5^\circ$

3 Open-Loop Control Strategy

We first investigated the effect of the prescribed periodic oscillating flap on the buffet suppression based on the CFD simulations. To make it convenient for operation, 20%-chord-length airfoil of the trailing is treated as flap without gap. The axis of the flap rotation is at 80% of the airfoil model chord. As the sketch

map shown in Figure 3, a positive flap rotation obtains when the flap rotates clockwise.

In the state of M = 0.7, Re = 3 10^6, and α=5.5° for a NACA 0012 airfoil. The control law is given as:

$$\beta(\tau) = A\sin(\omega_{flap}\tau + \varphi) = A\sin(n\omega_{flow}\tau + \varphi) \quad (1)$$

where A is the amplitude of the oscillating flap; ω_{flap} is the circular frequency of the oscillating flap, which is n times of the buffet frequency of ω_{flow}; τ is the nondimensional time and φ is the phase angle.

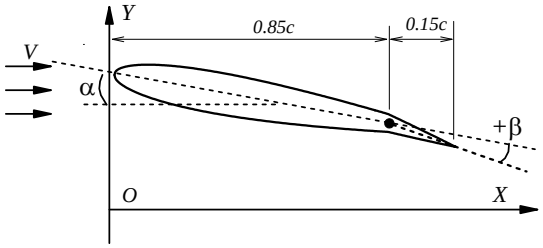

Figure 3. The schematic map of the actuator

In the case of flap with an oscillating frequency very close to the buffet frequency, it is found that the amplitudes of the lift and moment coefficients increase rapidly. The phase angle difference is also an important factor. Lift coefficient has about 70% decrease at phase angle difference towards 290 degrees with the oscillating amplitude of 2 degrees and frequency of 1.5 times of the buffet one (Figure 4). Above all, periodic oscillating flap may be a feasible open-loop strategy to decrease buffet loads with an appropriate and accessible combination of amplitude, frequency and phase angle difference. However, it is not advisable to obtain these combinations for different buffet states without any optimizing processes.

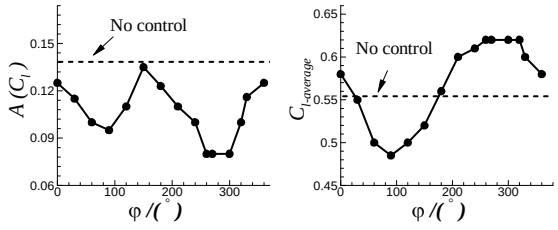

Figure 4 Amplitude and time-averaged lift coefficient with different phase angles difference at A=2° and n=1.5 by the open-loop strategy. The *dashed line* indicates the amplitude and time-averaged one without control.

4 Closed-Loop Control Strategy

As shown in Figure 3, a feedback model is set up. Based on the feedback signal of the lift coefficient, a closed-loop control law is proposed in this Section:

$$\beta(\tau) = \lambda[C_l(\tau - \Delta\tau) - C_{l0}], \quad (2)$$

where $\beta(\tau)$ is the angle of the flap rotation; C_{l0} is the balanced lift coefficient, $\Delta\tau$ is the delay time in nondimensional form; and λ is gain which is specified as a dimensionless parameter to control the flapping with the help of fluctuating $C_l(\tau)$.

4.1 Effect of Balanced Lift Coefficient

In the present work, the unstable steady solution [22, 23] is obtained by an iterative process. From Eq. (2), it can be assumed that if the given C_{l0} exactly equals the lift coefficient of the unstable steady solution (defined as C_{ls}), the stabilized flow will be exactly the same as the unstable steady flow, and the flap rotational angle will be zero. If a positive flap rotation is obtained, a nose-up effect is added on the airfoil to increase the lift coefficient, which means the assigned C_{l0} is larger than C_{ls}, and C_{l0} should be reduced in the next iteration. On the contrary, a negative flap rotation means a smaller assigned C_{l0}, and it should be increased in the next iteration. The flow chart of the iterative process is shown in Figure 5. Generally, the initial C_{l0} is assigned by the time-averaged lift coefficient. We then adjust the assigned value of C_{l0} according to the rotation of the flap. After some iteration, the unstable steady flow and the converged C_{l0} (equal to C_{ls}) can be achieved. Figure 6 shows responses of the typical iterative process. When the given C_{l0} is 0.553, the flap rotation is zero, which means the unstable steady solution is achieved and its lift coefficient is 0.553 at M = 0.7, Re = 3×10^6, $\alpha = 5.5°$.

The time-averaged and the unstable steady pressure contours are shown in Figure 7. They are very different. For the time-mean flow, the shock wave disappears and the distribution of pressure coefficients becomes smooth. However,

for the unstable steady flow, the shock wave remains 20% after the leading edge of the airfoil.

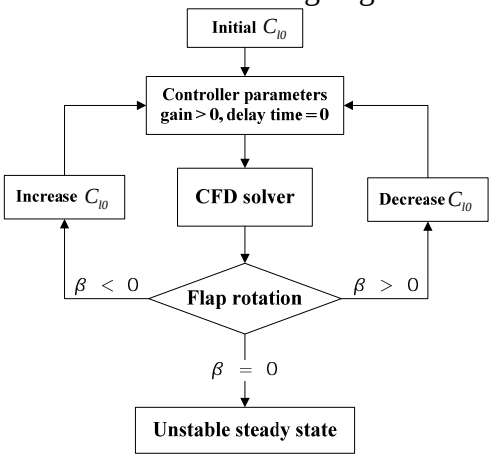

Figure 5. Flow chart of the iterative process to get the unstable steady solution

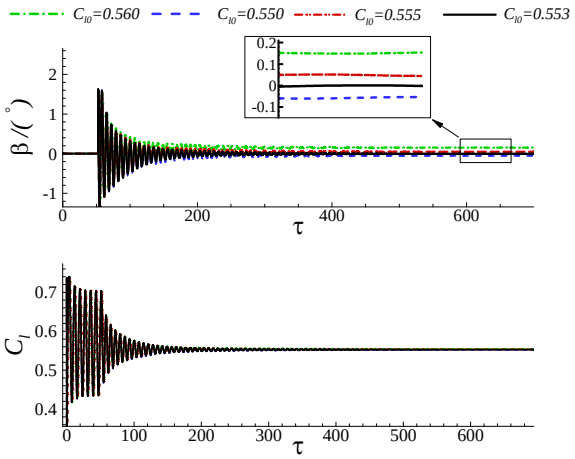

Figure 6. Time history of the lift coefficient with different C_{l0} at $\lambda = 0.3$ and $\Delta\tau = 0$

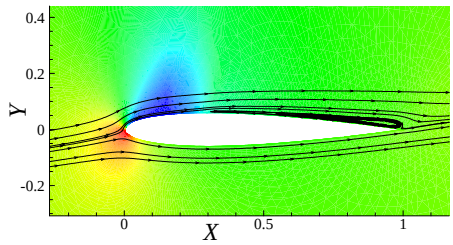

(a) Time-averaged flow field

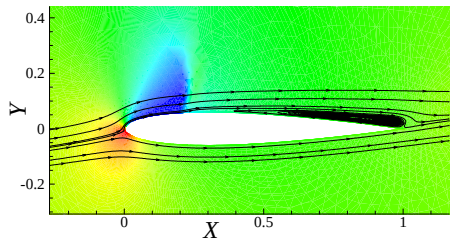

(b) Steady-state flow field

Figure 7. Comparison between the time-averaged and the steady pressure contours at *M=0.7*, *Re=3* 10^6, and $\alpha = 5.5^\circ$

4.2 Effect of Delay Time

The delay time can be given by the buffet period. To make it clear, we further transform the delay time into a phase. For example, the delay time of a half period is defined as $\Delta\tau = \frac{18}{36}T_0 = \frac{1}{2}2\pi = 180^\circ$, which means that the flap rotation response has a lag of 180 to the lift force. The present $\Delta\tau$ and T_0 are both nondimensional parameters which are nondimensionalized by the mean aerodynamic chord c and the free-stream sound speed a_∞. From another perspective, the delay time exceeding 180 can also be seen as the phase lead for the flap motion towards the lift response because of the approximately harmonic response, defined as φ_{lead}. For example, the delay time of $\Delta\tau = 31/36T_0$ is in equivalent to a phase lead of $\varphi_{lead} = 50^\circ$.

Figure 8 shows the time history of the responses with different delay times at $C_{l0} = 0.553$ and $\lambda = 0.15$. The stability of the closed-loop system can be completely changed at specified delay times. Figure 8 (b) demonstrates that when the delay time is $\Delta\tau = 9/36T_0$, the closed-loop system is more unstable with the amplitude of the lift coefficient 0.24, 60% larger than that of the stationary airfoil (0.17). At $\Delta\tau = 0$ and $\Delta\tau = 27/36T_0$, amplitudes of the lift force decrease by approximate 66% [Figures 8 (a) and 17(c)]. While at $\Delta\tau = 31/36T_0$ ($\varphi_{lead} = 50^\circ$), a stable flow field is achieved with a steady lift coefficient of 0.553 [Figure 8 (d)], equal to the given balanced lift coefficient. Therefore, buffet has been suppressed completely.

At delay time of $\Delta\tau = 0$ and $\Delta\tau = 27/36T_0$, as discussed in Figure 8, the closed-loop control can work but not in an ideal status. Within the range from $\Delta\tau = 30/36T_0$ to $\Delta\tau = 33/36T_0$ (from $\varphi_{lead} = 60^\circ$ to $\varphi_{lead} = 30^\circ$), where the mean delay time is about $\Delta\tau = 31/36T_0$ ($\varphi_{lead} = 50^\circ$), the cycles almost shrink to points in the arranged display scale. Therefore, buffet can be suppressed successfully in this range of delay time.

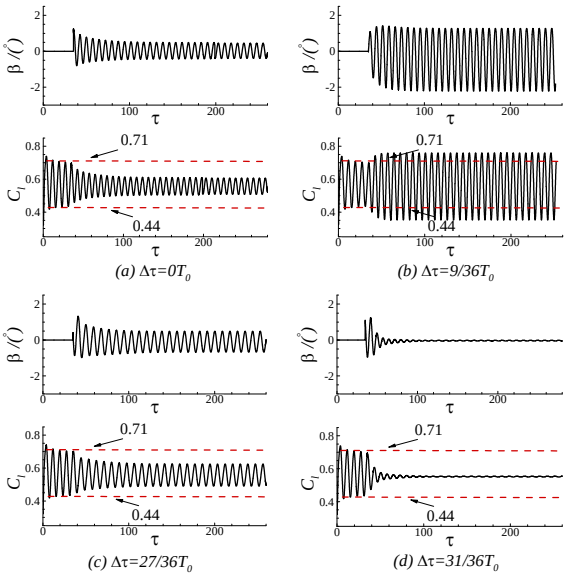

Figure 8. Time history of the responses with different delay time at $\lambda = 0.15$ and $C_{l0} = 0.553$

4.3 Suppression of Buffet Flow

Based on the above discussion on various parameters, the delay time plays an important role in the closed-loop control.

Figure 9 shows the effective control regions for different gains and delay time at *M=0.7*, $\alpha = 5.5^{\circ}$ and *Re=3 10*^{6}. The symbol " " indicates the control strategy is negative, enlarging the amplitude of the lift. The symbol " " indicates that the control strategy is positive to reduce the buffet unsteadiness rather than cancel it out; thus, it is called "positive but unsteady." The symbol " " indicates the control strategy is positive to suppress buffet completely, called "positive and steady." When $\lambda > 0$, the "positive and steady" region is from $\Delta\tau = 29/36T_0$ to $\Delta\tau = 34/36T_0$, where the phase lead is from 70° to 20° with a mean of 50°.

Four negative gains, $\lambda = -0.1$, $\lambda = -0.15$, $\lambda = -0.2$ and $\lambda = -0.3$, are also investigated with variable delay time. A positive gain can be changed to a negative one by reversing the flap rotation. Therefore, control regions of negative gains can approximately overlap those of positive gains moving them to the left by 180 .

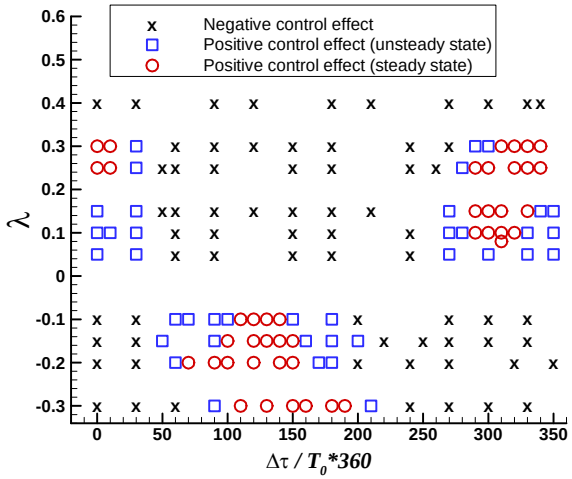

Figure 9. Effective control regions for different λ and $\Delta\tau$ at *M=0.7* $\alpha = 5.5^{\circ}$, *Re=3 10*^{6}

5 Conclusions

A numerical study is performed to investigate the effect of the open-loop and the closed-loop control on transonic buffet. The open-loop control is a prescribed periodic oscillating flap with 20% trailing edge. The closed-loop control is a time delayed control law with the feedback signal of the lift coefficient.

The open-loop periodic oscillating flap may be a feasible open-loop strategy to decrease buffet loads with an appropriate and accessible combination of amplitude, frequency and phase angle. However, it is not advisable to obtain these combinations for different buffet states without any optimizing processes.

Buffet at *M=0.7*, $\alpha = 5.5^{\circ}$, and *Re=3 10*^{6} can be suppressed completely with $\lambda = 0.25$ for $\Delta\tau = 0$, whereas for a delayed system at the optimal delay time of $\Delta\tau = 31/36T_0$ ($\varphi_{lead} = 50^{\circ}$), the gain can be reduced to $\lambda = 0.08$. Therefore, it is a valid closed-loop control strategy for transonic buffet suppression.

References

[1] Lee BHK. Self-sustained shock oscillations on airfoils at transonic speeds. *Progress of Aerospace Science*, Vol. 37, No. 2, pp 147-196, 2001.

[2] Hartmann A, Feldhusen A, Schröder W. On the interaction of shock waves and sound waves in transonic buffet flow. *Physics of Fluid*, Vol. 25, No. 2, pp 026101. 2013

[3] Doerffer P, Hirsch C, Dussauge JP. NACA0012 with Aileron, Unsteady Effects of Shock Wave Induced Separation, Springer, 2011.
[4] Jacquin L, Molton P, Deck S. Experimental study of shock oscillation over a transonic supercritical profile. *AIAA Journal* , Vol. 47, No. 9, pp 1985–1994, 2009.
[5] Sartor F, Mettot C, Sipp D. Stability, receptivity, and sensitivity analyses of buffeting transonic flow over a profile. *AIAA Journal*, Vol. 53, No. 7, pp 1980–1993, 2015.
[6] Barakos G, Drikakis D. Numerical simulation of transonic buffet flows using various turbulence closures. *Int J Heat Fluid Fl*, Vol. 21, No. 5, pp 620-626, 2000.
[7] Goncalves E, Houdeville R. Turbulence model and numerical scheme assessment for buffet computations. *Int J Numer Meth Fluid*, Vol. 46, No. 11, pp 1127-1152, 2004.
[8] Xiao Q, Tsai H, Liu F. Numerical study of transonic buffet on a supercritical airfoil. *AIAA Journal*, Vol. 44, No. 3, pp 620-628, 2006
[9] Raveh DE. Numerical study of an oscillating airfoil in transonic buffeting flows. *AIAA Journal*, Vol. 47, No. 3, pp 505-515, 2009.
[10] Zhang WW, Gao CQ, Liu YL, et al. The interaction between transonic buffet and flutter. *Nonlinear Dynamics*, Vol. 82, pp 1851–1865, 2015.
[11] Crouch JD, Garbaruk A, Magidov D. (2009) Origin of transonic buffet on airfoils. *Journal of Fluid Mechanics*, Vol. 628, pp 357-369, 2009.
[12] Gao CQ, Zhang WW, Liu YL, et al. Numerical study on the correlation of transonic single-degree-of-freedom flutter and buffet. *Sci China-Phys Mech Astron*, Vol. 58, pp 084701, 2015.
[13] Tian Y, Liu P, Li Z. Multi-objective optimization of shock control bump on a supercritical wing. *J Sci China Tech Sci*, Vol. 57, No. 1, pp 192-202, 2014.
[14] Eastwood J, Jarrett J. Toward designing with three-dimensional bumps for lift/drag improvement and buffet alleviation. *AIAA Journal*, Vol. 50, No. 12, pp 2882-2898, 2012.
[15] Ogawa H, Babinsky H, Pätzold M. Shock-wave/boundary-layer interaction control using three-dimensional bumps for transonic wings. *AIAA Journal*, Vol. 46, No. 6, pp 1442-1452, 2008.
[16] Huang J, Xiao Z, Liu J. Simulation of shock wave buffet and its suppression on an OAT15A supercritical airfoil by IDDES. *Sci China Phy Mechan Astron.*, Vol. 55, No. 2, pp 260-271, 2012.
[17] Titchener N, Babinsky H. Shock wave/boundary-layer interaction control using a combination of vortex generators and bleed. *AIAA Journal*, Vol. 51, No. 5, pp 1221-1233, 2013.
[18] Caruana D, Mignosi A, Robitaillié C. Separated flow and buffeting control. *Flow Turbulence and Combustion*, Vol. 71, pp 221-245, 2003.
[19] Caruana D, Mignosi A, Corrège M. Buffet and buffeting control in transonic flow. *Aerospace Science and Technology*, Vol. 9, No. 7, pp 605-616, 2005.
[20] Barbut G, Braza M, Hoarau Y. Prediction of transonic buffet around a wing with flap. Progress in Hybrid RANS-LES Modeling, Springer, 2010.
[21] Gao C, Zhang W and Ye Z. Numerical study on closed-loop control of transonic buffet suppression by trailing edge flap. *Computers and Fluid*s, Vol. **132**, No. 6, pp 32–45, 2016.
[22] Akervik E, Brandt L, Henningson D. Steady solutions of the Navier-Stokes equations by selective frequency damping. *Physics of Fluid*, Vol. 18, No. 6, pp 068102, 2006.
[23] Illingworth SJ, Morgans AS, Rowley CW. Feedback control of cavity flow oscillations using simple linear models. *Journal of Fluid Mechanics*, Vol. 709, pp 223-248, 2012.

Contact Author Email Address

Corresponding author: gao_800866@163.com

Copyright Statement